

## Characteristics of nanocrystalline CeO<sub>2</sub> thin films deposited on different substrates at room temperature

Lakshita Chaturvedi<sup>a,b</sup>, Smita Howlader<sup>a</sup>, Deepak Chhikara<sup>a</sup>, Preetam Singh<sup>a</sup>,  
Shobi Bagga<sup>b</sup> & K M K Srivatsa<sup>a\*</sup>

<sup>a</sup>Advanced Materials and Devices Division, CSIR-National Physical Laboratory, New Delhi 110 012, India

<sup>b</sup>Centre of Nanotechnology, Rajasthan Technical University, Kota 324 010, India

*Received 31 January 2017; accepted 6 May 2017*

Nanocrystalline cerium oxide (CeO<sub>2</sub>) thin films have been deposited over Si (100), Ni-W (200) and Al<sub>2</sub>O<sub>3</sub> (0006) substrates at room temperature by RF magnetron sputtering. The effect of RF sputtering power and deposition pressure on the optical and wettability properties of CeO<sub>2</sub> thin films has been investigated. X-ray diffraction patterns show the dominant single orientation (111) of CeO<sub>2</sub> thin films deposited on different substrates at 150 W applied RF power and 5 m Torr deposition pressure. But the value of full width at half maxima is found to be different on different substrates and varies in the range from 0.47°-0.65°. The corresponding crystallite size is also found to be varying from 16.94-12.46 nm. For these deposition parameters ellipsometer results reveal that the refractive index and band gap values are close to that of standard values. Thus, our results demonstrate that following sputtering process it is possible to deposit highly crystalline single oriented (111) CeO<sub>2</sub> thin films over different substrates even at room temperature simply by optimizing process parameters. Further, contact angle measurements indicate that all the deposited CeO<sub>2</sub> films show hydrophobic in nature.

**Keywords:** Nanocrystalline, CeO<sub>2</sub> thin films, Room temperature, Magnetron sputtering, Optical properties, Wettability

### 1 Introduction

Thin films of cerium oxide (CeO<sub>2</sub>) have received much attention because of their fascinating optical properties, such as high refractive index, good transmission in the visible and infrared regions and a wide band gap (3.2-3.6 eV), high refractive index (2.2-2.8) and high dielectric constant<sup>1-3</sup> (23-26). CeO<sub>2</sub> has cubic fluorite structure with a lattice parameter<sup>4,5</sup> of 5.411 Å. Its combined optical and electrical properties are highly desirable for applications such as electrochemical systems, fuel cells, capacitor material for dynamic random access memory and optoelectronic devices<sup>6</sup>. Also, thin film of CeO<sub>2</sub> is an attractive material because of its potential applicability as passive counter electrode in electrochromic smart windows<sup>7</sup>. The Ce ion in the CeO<sub>2</sub> film exhibits both +3 and +4 oxidation states, which are suitable for valency change switching process<sup>8-10</sup>. Further, CeO<sub>2</sub> has a good structural compatibility with YBCO superconductor and Si and also has an excellent thermal and chemical stability with Ni, and thus serves as a good buffer layer for superconductor, semiconductor and piezoelectric films over metal substrates<sup>11-13</sup>.

The properties of materials like structural, optical, electrical, mechanical, catalytic etc. get changed with reducing the grain size from bulk to nanocrystalline thin films and play an important role in the potential device applications. The optical properties of the CeO<sub>2</sub> films have been reported by several workers providing different values for the refractive index ( $n$ ) and the optical band gap ( $E_g$ ) in the range 1.78-2.6 and 2.0-3.6 eV, respectively<sup>5,14-16</sup>.

Wettability is a fundamental property of a solid surface, which has a variety of practical applications in the fields of daily life, industry, and agriculture. Wettability is the ability of solid surface to reduce the surface tension of a liquid in contact with the surface such that it spreads over the surface and wets the surface<sup>17,18</sup>. Many materials surfaces exhibit hydrophobic/hydrophilic nature. Hydrophobic characteristics have many research applications in corrosion prevention, liquid conveyance, self-cleaning surfaces, and among other fields<sup>19-22</sup>. The specific interesting properties of hydrophilic coatings are less dirt, easy to clean, antifogging and inhibition of growth for vegetation and bacteria<sup>23,24</sup>. CeO<sub>2</sub> is mostly studied one with regard to its wetting properties due to its abundant availability and low cost compared to other rare earth oxides (REOs)<sup>25</sup>. It is to be noted that the

\*Corresponding author (E-mail: kmks@nplindia.org)

surface chemistry of the materials plays a significant role in determining the wettability, which in turn depends on the deposition technique and related deposition parameters. Recently Khan *et al.*<sup>25</sup> have reported that how excess surface oxygen in REOs can negatively impact hydrophobicity. Singh *et al.*<sup>26</sup> have reported that the wettability of the sputtered CeO<sub>2</sub> films varies from hydrophobic to hydrophilic with respect to increasing substrate temperature on Si substrate. However, the effect of other process parameters and the role of the substrates on the wettability of room temperature deposited CeO<sub>2</sub> thin films were not reported. Thus, all the above discussion indicates that the properties of deposited/grown CeO<sub>2</sub> thin films depend on the deposition technique and the related process parameters.

Keeping in view of the wide range of applications of CeO<sub>2</sub> many workers have tried to deposit CeO<sub>2</sub> thin films by variety of techniques, viz, E-beam evaporation<sup>27</sup>, RF/DC magnetron sputtering<sup>16,26</sup>, cathodic electrodeposition<sup>28,29</sup>, pulsed laser deposition<sup>5,30</sup>, laser molecular-beam epitaxy<sup>6</sup>, chemical vapor deposition<sup>31</sup>, sol-gel<sup>19,32,33</sup> and so on, and reported the structural and optical properties. Among various deposition techniques, RF/DC magnetron sputtering has been recognized as a promising versatile technique for the deposition of stoichiometric film of metal oxides. Its main advantages are good adhesion to substrates, and high density and homogeneity of deposited films. Moreover it permits large scale deposition of high quality films at high deposition rates<sup>34,35</sup>. In most of the cases CeO<sub>2</sub> thin films have been deposited/annealed at high temperatures to achieve high quality films. However, our present work shows it is possible to achieve the high quality nanocrystalline CeO<sub>2</sub> thin films on different substrates even at room temperature. We have used the RF magnetron sputtering technique for the deposition of CeO<sub>2</sub> thin films at different process parameters and the related results are presented in this paper.

## 2 Experimental Details

CeO<sub>2</sub> ceramic target (purity 99.99%) and Ar (purity 99.999%) gas have been used for the preparation of nanocrystalline CeO<sub>2</sub> thin films on Si, Ni-W and Al<sub>2</sub>O<sub>3</sub> substrates. Before deposition all the substrates were first degreased in boiling trichloroethylene (TCE), followed by acetone methanol, and de-ionized water cleaning. In case of Si, the substrate was dipped in 10% HF for 10 s to remove the native SiO<sub>2</sub> layer, followed by rinsing in de-ionized water. All chemicals used for

cleaning the substrates were semiconductor grade (Merck Ltd).

In-house designed and fabricated downstream RF magnetron sputtering system was used for the present work. A turbo-based pumping system, backed by roots and rotary pumps, was used to achieve a base pressure below  $3 \times 10^{-6}$  Torr. The distance between the sputtering target and substrate was fixed at 3 inch. The deposition pressure in the vacuum chamber was measured by a compact process ion gauge (Pfeiffer) and the gas flow rate was accurately controlled by mass flow controllers (Aalborg, model: GFC-17). All the CeO<sub>2</sub> thin films were deposited at room temperature and the applied RF sputtering power and deposition pressure were varied from 100 to 150 W and 5 to 30 mTorr, respectively.

The structural properties of CeO<sub>2</sub> thin films were characterized by an X-ray diffractometer (Bruker, Germany, model: D8-Avalance), using Cu K $\alpha$  radiation at 1.54 Å in  $\theta$ -2 $\theta$  geometry. The optical properties of CeO<sub>2</sub> thin films were studied by spectroscopic ellipsometer (J A Woollam, model: VASE32) and the optical parameters were calculated in the wavelength range 250-1200 nm, for the incident angles 55°, 65° and 75°. The contact angles of CeO<sub>2</sub> thin films were recorded by Sessile drop method (Data physics model OCA15EC) to determine the wetting behaviour of deposited films.

## 3 Results and Discussion

Figure 1 shows the X-ray diffraction (XRD) pattern of nanocrystalline CeO<sub>2</sub> thin films deposited on Si (100) substrate at room temperature. At 100 W RF power and 30 mTorr deposition pressure the film shows (111) and (220) peaks of CeO<sub>2</sub> with poor crystallinity and no preferred orientation was observed. Keeping the RF power fixed at 100 W and decreasing the deposition pressure to 5 mTorr, it shows single peak of (111) orientation with high crystalline quality. Similarly, at 150 W RF power and 5 mTorr pressure the film shows highly intense peak of (111) orientation, while at 30 mTorr it shows multiple peaks with poor crystallinity. The formation of both (111) and (220) orientations and poor crystallinity at high pressure can be explained on the basis of the relation between sputtering pressure and mean free path of gas molecules<sup>36</sup>. The mean free path of the sputtering gas molecule is given by:

$$\lambda = 2.33 \times 10^{-20} \frac{T}{P \delta_m^2} \quad \dots (1)$$

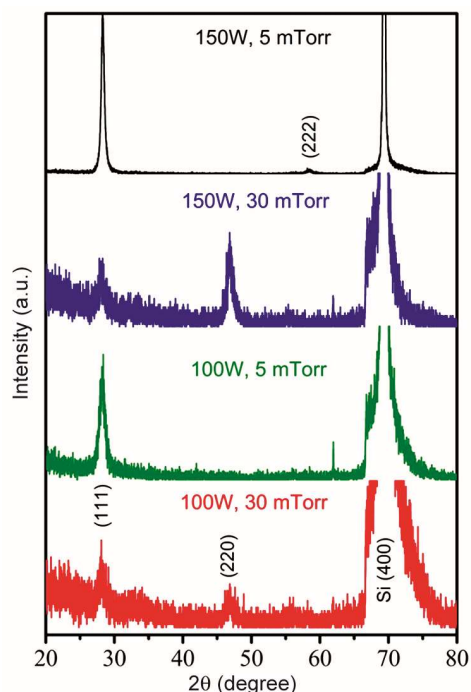


Fig. 1 — X-ray diffraction pattern of CeO<sub>2</sub> thin films deposited on Si (100) substrate at different deposition parameters.

where  $T$ ,  $P$  and  $\delta_m$  are the temperature, pressure and molecule diameter, respectively. The above equation indicates that the mean free path is inversely proportional to the pressure. Thus as the deposition pressure increases (30 mTorr) there is a reduction in mean free path, which increases the collision frequency, and would reduce the sputtering rate and result in change in the orientation and crystallinity. Due to this reason, the considerable change in the crystallinity has not observed at high deposition pressure with increasing the RF power. While, at low deposition pressure of 5 mTorr, the less number of sputtered molecules will undergo collisions with the sputtering gas, resulting in retention of the kinetic energy of the sputtered molecules. Hence more number of sputtered molecules reaches the surface of substrate with high kinetic energy and their mobility increases on the substrate surface, leading to more crystallinity with increasing the RF power to 150 W. This indicates that the crystallographic orientation of the films can be controlled by sputtering parameters, i.e., sputtering power and pressure has a great influence on the structural properties of the CeO<sub>2</sub> films.

The crystallite size ( $d$ ) of the films was calculated using the well known Scherer's formula<sup>37</sup> as follow:

$$d = \frac{0.9\lambda}{\beta \cos\theta} \quad \dots (2)$$

Table 1 — Calculated parameters of nanocrystalline CeO<sub>2</sub> thin films deposited on Si substrate

Calculated parameters	100 W		150 W	
	30 mTorr	5 mTorr	30 mTorr	5 mTorr
FWHM (degree)	0.82	0.72	0.82	0.47
Crystallite size (nm)	9.85	11.25	9.85	16.94
Lattice parameter (nm)	0.549	0.545	0.550	0.545

where  $\lambda$ ,  $\theta$  and  $\beta$  are the X-ray wavelength (1.54Å), Bragg diffraction angle and full width at half-maximum (FWHM), respectively. The calculated crystallite size, FWHM and lattice constant along (111) peak and the values are shown in Table 1. The value of FWHM was found to decrease from 0.72° to 0.47° and the corresponding crystallite size was increased from 11.22 nm to 16.94 nm with increasing the RF power from 100 to 150 W at 5 mTorr. On the other hand at 30 mTorr deposition pressure no considerable change is observed with increasing the RF power from 100 W to 150 W. The crystalline formation of deposited film occurs due to either substrate heating or the energy supplied by the energetic Ar<sup>+</sup> ions bombardment during sputtering process<sup>31</sup>. In the present experiment, we have not used the substrate heating during the deposition. Thus the energetic sputtered particles impinging on the film surface are the only reason for crystallization of CeO<sub>2</sub> thin films.

In order to see the influence of substrate type we have also deposited the nanocrystalline CeO<sub>2</sub> thin films over flexible Ni-W (200) and Al<sub>2</sub>O<sub>3</sub> (0006) substrates. The deposition pressure was fixed at 5 mTorr and RF power varies from 100 W to 150 W as shown in the XRD pattern in Fig. 2. All the deposited films show only (111) orientation at 100 W RF power and the intensity of (111) peak increased as the RF power increases further to 150 W. These results are similar to the nanocrystalline thin films deposition on Si substrate at same deposition conditions. We have calculated the crystallite size, FWHM and lattice constant along (111) peak and the values are shown in Table 2. The value of FWHM was found to decrease from 0.75 to 0.51° and from 1.25 to 0.65° and the corresponding crystallite size was increased from 10.72 to 15.60 nm and from 6.40 to 12.46 nm for the films deposited on Ni-W and Al<sub>2</sub>O<sub>3</sub> substrates, respectively, with increasing the RF power from 100 to 150 W.

The optical properties of CeO<sub>2</sub> thin films deposited on Si substrate were studied by spectroscopic ellipsometer (SE) in the wavelength range of 250-1200 nm. SE measurements provide the data related to the ellipsometer angle  $\Psi$  and phase  $\Delta$  with respect to

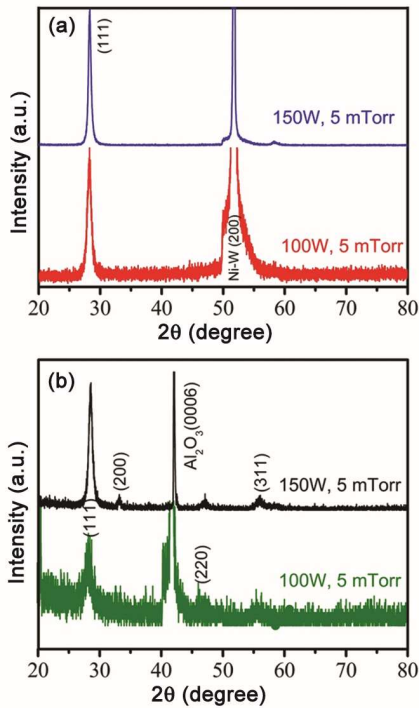


Fig. 2 — X-ray diffraction pattern of CeO<sub>2</sub> thin films deposited on (a) biaxially textured Ni-W and (b) Al<sub>2</sub>O<sub>3</sub> substrate at different deposition parameters.

Table 2 — Various calculated parameters of nanocrystalline CeO<sub>2</sub> thin films deposited on biaxially textured Ni-W and Al<sub>2</sub>O<sub>3</sub> substrate

CeO <sub>2</sub> /Substrate	Ni-W		Al <sub>2</sub> O <sub>3</sub>	
	5 mTorr			
Calculated parameters	100 W	150 W	100 W	150 W
FWHM (degree)	0.75	0.51	1.25	0.65
Crystallite size (nm)	10.72	15.60	6.40	12.46
Lattice parameter	0.547	0.545	0.543	0.545

wavelength ( $\lambda$ ) or photon energy. It is a non-destructive model fitting based technique, which minimizes the difference between measured experimental and calculated fitting values as a function of wavelength. The experimental data has been fitted using Tauc-Lorentz (TL) model for the air/CeO<sub>2</sub>/Si structure which takes into account the film thickness and contribution of the substrate<sup>15</sup>. The solid line in the Fig. 3 represents the model-fit data and it can be seen that all the features present in the experimental spectra are reproduced by the model fit. The fitting parameters within the parametric dispersion model yields thickness of CeO<sub>2</sub> thin films and is summarized in Table 3. It can be seen that the thicknesses of CeO<sub>2</sub> thin films strongly depend on the deposition parameters. The thickness increases with increasing the RF power from 100 to 150 W at both the deposition pressures 5 mTorr and 30 mTorr.

The reason may be the same as we have explained above that the growth rate depends on the deposition conditions and should be different at different deposition parameters that results the change in film thickness.

Figure 4(a, b) represents the refractive index ( $n$ ) as a function of wavelength in the range of 250-1200 nm as obtained from the corresponding ellipsometric data of CeO<sub>2</sub> thin films deposited on Si substrate. The observed value of  $n$  at 650 nm wavelength of deposited CeO<sub>2</sub> films varied from 2.36 to 2.42 eV, which are well matched to the reported values of  $n$  for CeO<sub>2</sub> thin films (2.2-2.6) and single crystal (2.4-2.56) in the literature<sup>38-40</sup>. The reason for the variation of  $n$  may be due to the change in packing density and crystallinity at different deposition conditions as observed from XRD results. At 30 mTorr, the refractive index decreases with the increase in power from 100 to 150 W. This is because, at 100 W the growth rate is low as a result the collision frequency is also low even the pressure is high. So the packing density may be better at 100 W than 150 W RF power. While at 5 mTorr the packing density and crystallinity is improved with increasing the power from 100 to 150 W due the low collision frequency at low pressure. This improves the value of refractive index.

The extinction coefficient ( $k$ ) of CeO<sub>2</sub> films deposited on Si substrate at different process parameters is shown in Fig. 4(c, d). Extinction coefficient is the imaginary part of the complex index of refraction, which also relates to light absorption. It defines how strongly a substance absorbs light at a given wavelength and is directly related to the absorption coefficient as follow<sup>41</sup>:

$$k = \alpha\lambda/4\pi \quad \dots (3)$$

where  $\alpha$  and  $\lambda$  are absorption coefficient and wavelength, respectively. It is clear from the graphs that all the CeO<sub>2</sub> films show absorption in UV region, but in the visible and IR range the values of  $k$  are negligible, i.e., almost zero. These results indicate that the CeO<sub>2</sub> films are highly transparent in the visible range.

According to inter-band absorption theory, the optical band gap of the films can be calculated using the Tauc relation<sup>42</sup> as following:

$$ahv = A(hv - E_g)^n \quad \dots (4)$$

where  $A$ ,  $E_g$ ,  $h\nu$  and  $n$  are the probability parameter for the transition, band gap of the material, incident photon energy and the transition coefficient ( $n = 2$  for

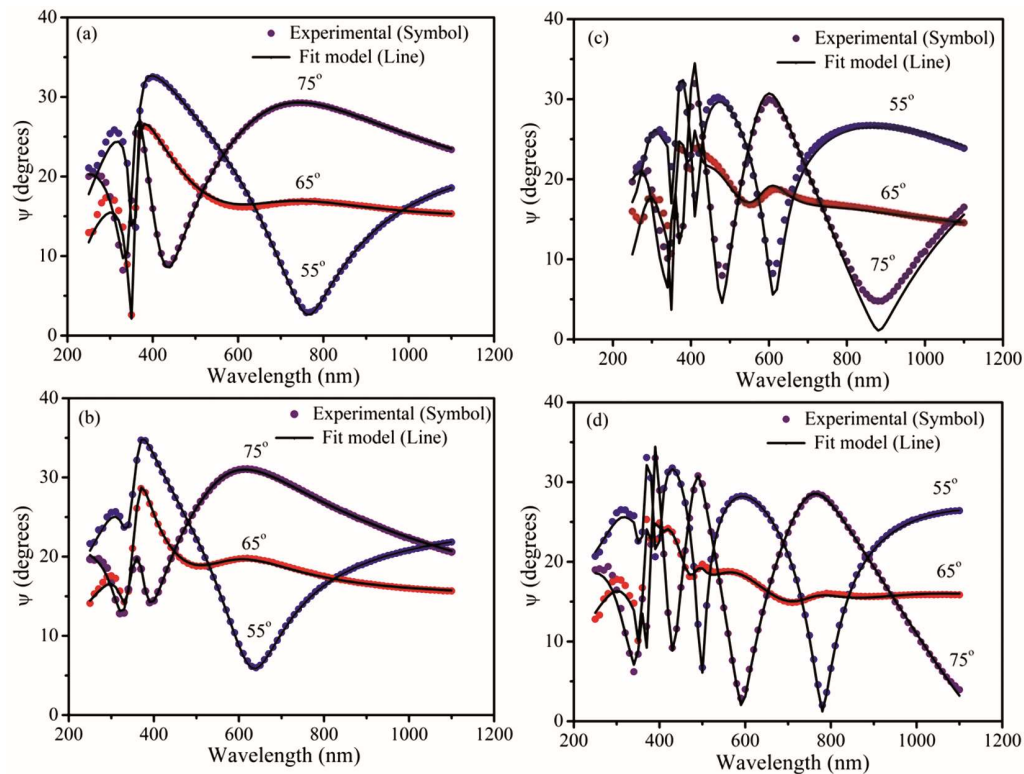


Fig. 3 — Experimental and model fitted ellipsometric parameter ( $\Psi$ ) of  $\text{CeO}_2$  thin films deposited at (a) 100 W, 30 mTorr, (b) 100 W, 5 mTorr, (c) 150 W, 30 mTorr and (d) 150 W, 5 mTorr, respectively.

Table 3 — Calculated optical parameters of nanocrystalline  $\text{CeO}_2$  thin films deposited on Si substrate

Calculated parameters	30 mTorr		5 mTorr	
	100 W	150 W	100 W	150 W
Thickness (nm)	84.98	207.47	69.31	260.36
Refractive index at 650 nm	2.40	2.37	2.36	2.42
Optical band gap (eV)	3.22	3.11	3.19	3.20

indirect and  $n = 1/2$  for direct band gap), respectively. The absorption coefficient  $\alpha$  has been extracted from the ellipsometric data after model fitting. Here, the indirect band gap of the  $\text{CeO}_2$  films was evaluated by extrapolating the straight line part of the curves  $(\alpha h\nu)^{1/2}$  as shown in Fig. 5. The calculated values of band gap of  $\text{CeO}_2$  thin films was found in the range 3.11 to 3.22 eV and are shown in Table 4. The reason may be due to the fact that packing density and crystallinity are changed with deposition conditions and these results are in agreement with the XRD results and refractive index values. Bueno *et al.*<sup>43</sup> have observed the single oriented nanocrystalline  $\text{CeO}_2$  films on pyrex substrate at room temperature by sputtering technique with the refractive index and band gap values 2.25-2.4 and 3.1 eV, respectively, and is supporting our present results. Thus, our results demonstrate that high quality

(111) single oriented nanocrystalline  $\text{CeO}_2$  thin films can be deposited over different substrates even at room temperature by simply optimizing the power and pressure following sputtering technique.

Wettability of solid surfaces is governed by their surface free energies and surface geometrical structures. The water contact angle (WCA) on the surface of interest<sup>44</sup> indicates the wetting nature of the surface whether it is hydrophobic (if the contact angle is  $\theta > 90^\circ$ ) or hydrophilic<sup>45</sup> (if the contact angle  $\theta$  is  $< 90^\circ$ ). Wetting properties of nanocrystalline  $\text{CeO}_2$  thin films are studied by contact angle measurement. The contact angle of  $\text{CeO}_2$  thin film deposited on Si substrate is shown in Fig. 6. The results show increasing hydrophobicity with the increasing deposition pressure from 5 to 30 mTorr at both RF powers (100 W and 150 W) and the results are summarized in Table 4. The contact angle value of thin film deposited at 100 W increased from  $98.75^\circ$  to  $108.64^\circ$  with increasing the deposition pressure from 5 to 30 mTorr. While the contact angle value at 150 W increased from  $103.12^\circ$  to  $108.68^\circ$  with increasing the deposition pressure (5 to 30 mTorr). The increase in the contact angle, i.e., the hydrophobic nature may be due to the fact that packing density and crystallinity are

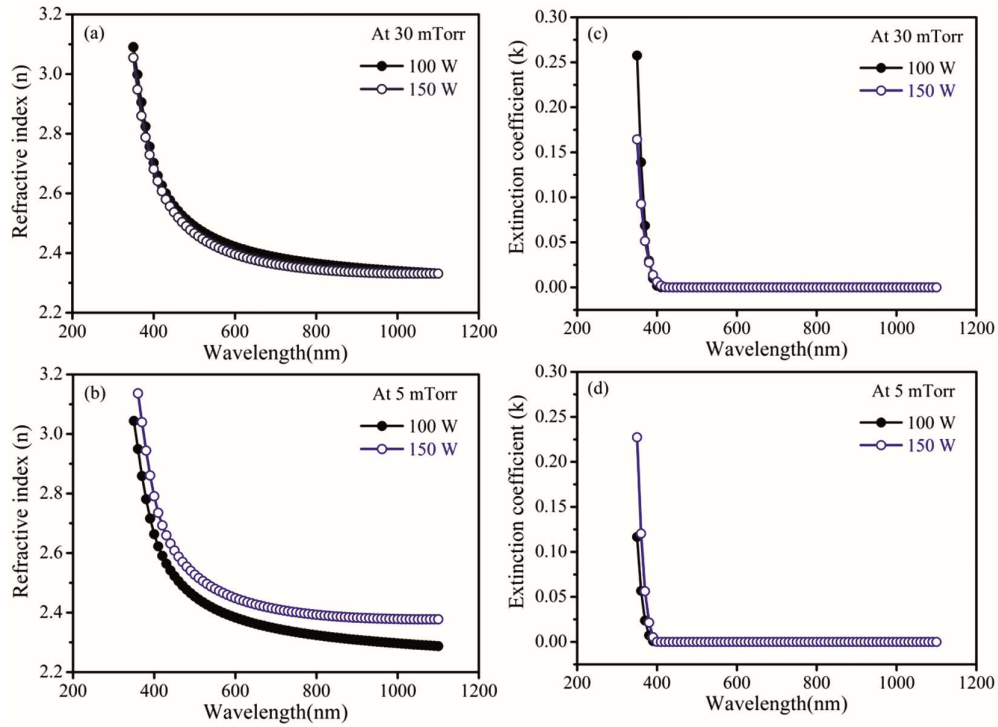


Fig. 4 — Dispersion behaviour of refractive index ( $n$ ) and extinction coefficient ( $k$ ) of CeO<sub>2</sub> thin films deposited on Si substrate at different deposition conditions.

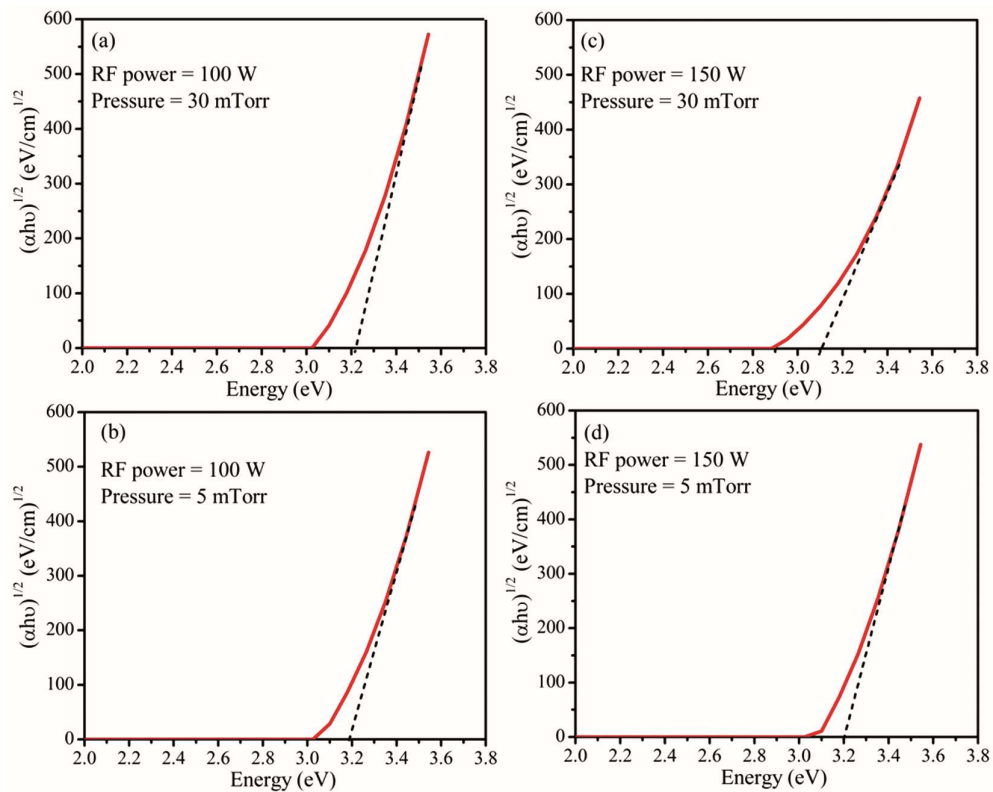


Fig. 5 —  $(\alpha h\nu)^{1/2}$  vs  $h\nu$  plots of the CeO<sub>2</sub> thin films deposited on Si substrate at different deposition conditions.

Table 4 — Contact angle measurement images of CeO<sub>2</sub> thin films deposited on Si, Al<sub>2</sub>O<sub>3</sub> and Ni-W substrates at different deposition conditions

CeO <sub>2</sub> /Substrate	100 W		150 W	
	30 mTorr	5 mTorr	30 mTorr	5 mTorr
Si	108.64°	98.75°	108.68°	103.12°
Al <sub>2</sub> O <sub>3</sub>	112.77°	99.45°	104.25°	98.32°
Ni-W	99.96°	91.40°	109.39°	97.94°

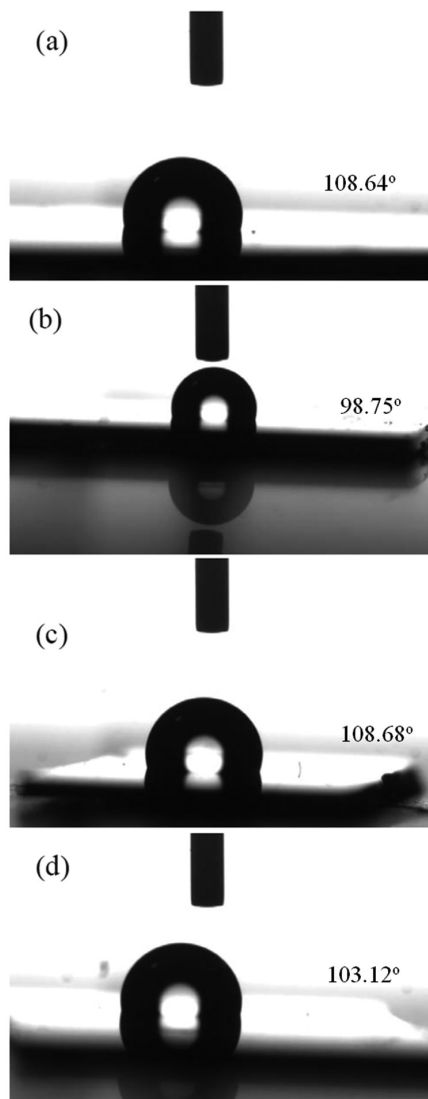


Fig. 6 — Contact angle images of CeO<sub>2</sub> films deposited on Si substrate at (a) 100 W, 30 mTorr, (b) 100 W, 5 mTorr, (c) 150 W, 30 mTorr and (d) 150 W, 5 mTorr, respectively.

changed with the deposition conditions as we have explained in the XRD and optical results.

For the sake of comparison, we have also measured the contact angle of CeO<sub>2</sub> thin films deposited on Ni-W and Al<sub>2</sub>O<sub>3</sub> substrates (images are not shown here) and the results are summarized in Table 4. It is

observed that on all the substrates the CeO<sub>2</sub> thin films show only hydrophobic nature. The contact angle was found to increase with increasing deposition pressure at both RF powers (at 100 W and 150 W). But the contact angle at the same deposition parameters was found different on all three substrates. For example at 100 W and 5 mTorr the contact angle was 98.75°, 112.77° and 91.4° of CeO<sub>2</sub> thin film deposited on Si, Al<sub>2</sub>O<sub>3</sub> and Ni-W substrates, respectively. Thus, these contact angle measurement results further confirm that along with structural and optical, the wettable properties of CeO<sub>2</sub> films are dependent on the process parameters as well as on the type/nature of substrate.

#### 4 Conclusions

In summary, we have deposited nanocrystalline CeO<sub>2</sub> thin films on different substrates (Si, Al<sub>2</sub>O<sub>3</sub> and Ni-W) at room temperature by RF magnetron sputtering technique. The structural, optical and wettable properties of the deposited thin films were investigated at different process parameters. The XRD studies of the as deposited CeO<sub>2</sub> thin films at 150 W RF power and 5 mTorr deposition pressure show predominant (111) orientation on all the substrates. Optical properties extracted from ellipsometer results reveal that the refractive index (2.42) and band gap (3.2 eV) values are at par with that of standard values. Contact angle measurements indicated that all the deposited CeO<sub>2</sub> thin films are of hydrophobic nature. Thus, our results demonstrate that single oriented (111) nanocrystalline CeO<sub>2</sub> thin films can be deposited over different substrates even at room temperature simply by optimizing the sputtering process parameters.

#### Acknowledgement

The authors are grateful to the Director, CSIR-National Physical Laboratory, New Delhi, India for his continuous encouragement and support during this work. Authors would like to fully acknowledge the help of Dr N Vijiyan and Dr V V Agrawal for XRD and contact angle measurements, respectively. The financial support provided by Department of Science and Technology (DST) through SERB, New Delhi, India with reference No: SB/EMEQ-040/2014 (Project No: GAP150332) is gratefully acknowledged.

#### References

- 1 Chen C H, Chang I Y K, Lee J Y M & Chiu F C, *Appl Phys Lett*, 92 (2008) 043507.
- 2 Arul N S, Mangalaraj D & Kim T W, *Appl Phys Lett*, 102 (2013) 223115.

- 3 Kim W H, Maeng W J, Kim M K, Gatineau J & Kim H, *J Electrochem Soc*, 158 (2011) 217.
- 4 Gschneider K A & Eyring L, *Handbook on the physics and chemistry of rare earths*, (North Holland: Amsterdam), 1979.
- 5 Balakrishnan G, Sundari S T, Kuppusami P, Mohan P C, Srinivasan M P, Mohandas E, Ganesan V & Sastikumar D, *Thin Solid Films*, 519 (2011) 2520.
- 6 Chen J & Meng D, *Integr Ferroelectr*, 138 (2012) 145.
- 7 Koo H, Shin D, Bae S H, Ko K E, Chang S H & Park C, *J Mater Eng Perform*, 23 (2014) 402.
- 8 Panda D, Dhar A & Ray S K, *IEEE Trans Nano Technol*, 11 (2012) 51.
- 9 Waser R & Aono M, *Nature Mater*, 6 (2007) 833.
- 10 Singh P, Srivatsa K M K, Barvat A & Pal P, *Curr Appl Phys*, 16 (2016) 1388.
- 11 Xiong J, Chen Y, Qiu Y, Tao B, Qin W, Cui X, Tang J & Li Y, *Supercond Sci Technol*, 19 (2006) 1068.
- 12 Zhao Y & Grivel J C, *Cryst Eng Comm*, 15 (2013) 3816.
- 13 Lee H G, Lee Y M, Shin H S, Kim C J & Hong G W, *Mater Sci Eng B*, 90 (2002) 20.
- 14 Nie J C, Hua Z Y, Dou R F & Tu Q Y, *J Appl Phys*, 103 (2008) 054308.
- 15 Patsalas P, Logothetidis S & Metaxa C, *Appl Phys Lett*, 81 (2002) 466.
- 16 Singh P, Srivatsa K M K & Das S, *Adv Mater Lett*, 6 (2015) 371.
- 17 Quere D, *Rep Prog Phys*, 68 (2005) 2495.
- 18 Papadopoulos P, Mammen L, Deng X, Vollmer D & Butt H J, *Proc Natl Acad Sci USA*, 110 (2013) 3254.
- 19 Shirlcliffe N J, McHale G, Newton M I & Perry C C, *Langmuir*, 19 (2003) 5626.
- 20 Marmur A, *Langmuir*, 20 (2004) 3517.
- 21 Meuler A J, Smith J D, Varanasi K K, Mabry J M, McKinley G H & Cohenet R E, *ACS Appl Mater Interfaces*, 2 (2010) 3100.
- 22 Bahadur V & Garimella S V, *Langmuir*, 23 (2007) 4918.
- 23 Parkin I P & Palgrave R G, *J Mater Chem*, 15 (2005) 1689.
- 24 Fujishima A, Rao T N & Tryk D A, *J Photochem Photobiol C: Photochem Rev*, 1 (2000) 1.
- 25 Sami K, Gisele A, Bilge Y & Varanasi K K, *Appl Phys Lett*, 106 (2015) 061601.
- 26 Srivatsa K M K, Singh P & Das S, *Adv Mater Lett*, 6 (2015) 883.
- 27 Singh P & Srivatsa K M K, *Indian J Pure Appl Phys*, 54 (2016) 359.
- 28 Shi F, Wang Z & Zhang X, *Adv Mater*, 17 (2005) 1005.
- 29 Hsieh C T, Yang S Y & Lin J Y, *Thin Solid Films*, 518 (2010) 4884.
- 30 Khorasani M, Mirzadeh H & Kermani Z, *App Surf Sci*, 242 (2005) 339.
- 31 Huang L, Lau S P, Yang H Y, Leong E S P, Yu S F & Praver S, *J Phys Chem*, 109 (2005) 7746.
- 32 Hikita M, Tanaka K, Nakamura T, Kajiyama T & Takahara A, *Langmuir*, 21 (2005) 7299.
- 33 Rao A V, Latthe S S, Nadargi D Y, Hirashima H & Ganesan V, *J Colloid Interface Sci*, 332 (2009) 484.
- 34 Zhang Y, Ma X, Chen P & Yang D, *J Cryst Growth*, 300 (2007) 55.
- 35 Singh P, Kumar A & Kaur D, *Physica B*, 403 (2008) 3769.
- 36 Singh P, Chawla A K, Kaur D & Chandra R, *Mater Lett*, 61 (2007) 2050.
- 37 Cullity B D, *Elements of X-ray diffraction*, (Addison-Wesley: Reading, MA), 1970.
- 38 Singh P & Kaur D, *Physica B*, 405 (2010) 1258.
- 39 Eglitis R I, Shi H & Borstel G, *Surf Rev Lett*, 13 (2006) 149.
- 40 Cao G, *Nanostructures & nanomaterials: Synthesis, properties & applications*, (Imperial College Press: London), 2004.
- 41 Ozer N, *Sol Energy Mater Sol Cells*, 68 (2001) 391.
- 42 Tauc J, *Amorphous and liquid semiconductor*, (Plenum Press: New York), 1974.
- 43 Bueno R M, Martines-Duart J M, Ndez-Velez M & Vazquez L, *J Mater Sci*, 32 (1997) 1861.
- 44 Fowkes F, *Wettability and Adhesion*, (American Chemical Society), 1964.
- 45 Blossey R, *Nature Mater*, 2 (2003) 301.